DOI: 10.1002/anie.201000449

Defensive Sesterterpenoids

Glandular Trichomes of *Leucosceptrum canum* Harbor Defensive Sesterterpenoids**

*Shi-Hong Luo, Qian Luo, Xue-Mei Niu, Ming-Jin Xie, Xu Zhao, Bernd Schneider, Jonathan Gershenzon, and Sheng-Hong Li**

Dedicated to Professor Han-Dong Sun on the occasion of his 70th birthday

Plant trichomes (both glandular and nonglandular) are epidermal protuberances that have been found on the surfaces of aerial organs of most terrestrial plants, including angiosperms, gymnosperms, and bryophytes.[1] Glandular trichomes of plants often produce copious secondary metabolites with a wide range of structures and biological properties, including alkaloids, phenolics, and terpenoids.[2,3] These substances are secreted from glandular trichomes onto the plant surface or stored within the gland cavity,[1,2] and are often thought to serve as defenses against herbivores, but good evidence for their protective roles is usually lacking.

Among the plants of southwest China, *Leucosceptrum canum* Smith, a shrub or small tree belonging to the family Labiatae (=Lamiaceae), is densely covered with gray or yellowish trichomes. This species is perhaps the largest (up to 10 m high[4]) and so far the only colored nectar plant[5] of all Labiatae species, and is found from the Himalayas to the southwest of China.[5,6] This plant is rarely attacked by herbivores and only occasionally by pathogens. We studied *L. canum* to identify the constituents of the glandular trichomes and investigate their possible function in plant defense.

Numerous gray or yellowish trichomes, both glandular and nonglandular, cover the buds, flowers, and especially the leaves of *L. canum* (Figure 1 A and B). Under the scanning electron microscope, the nonglandular trichomes appear as stellate structures, distributed on the stems, leaves (especially young leaves), buds, and bracts (Figure 1 C and D). The glandular trichomes include two main types: peltate and capitate trichomes. The peltate glandular trichomes have a

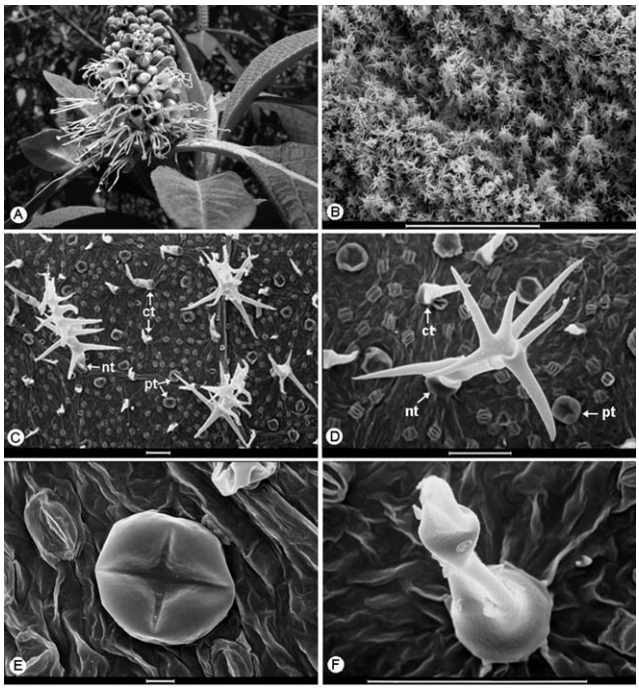

Figure 1. A) *L. canum* plant in bloom. B–F) Scanning electron micrographs showing trichomes on the abaxial and adaxial leaf surfaces, the caulicle, and the surface of bracts. B) Numerous trichomes on the abaxial leaf surface. Scale bar: 1 mm. C) Three major types of trichomes, nonglandular trichomes (nt), peltate glandular trichomes (pt), and capitate glandular trichomes (ct), on the abaxial leaf surface. Scale bar: 100 μm. D) Branched nonglandular trichome on the abaxial leaf surface, surrounded by peltate and capitate glandular trichomes. Scale bar: 100 μm. E) Peltate glandular trichome on the abaxial leaf surface. Scale bar: 10 μm. F) Capitate glandular trichome on the abaxial leaf surface. Scale bar: 100 μm.

[*] S.-H. Luo, Dr. Q. Luo, X. Zhao, Prof. Dr. S.-H. Li
State Key Laboratory of Phytochemistry and Plant Resources in West China, Kunming Institute of Botany, Chinese Academy of Sciences
Lanhei Road 132, Kunming 650204 (P. R. China)
Fax: (+86) 871-522-3035
E-mail: shli@mail.kib.ac.cn
Homepage: http://www.kib.ac.cn
Prof. Dr. X.-M. Niu
Key Laboratory for Conservation and Utilization of Bioresources
Yunnan University, Kunming (P. R. China)
Prof. Dr. M.-J. Xie
Department of Chemistry, Yunnan University, Kunming (P. R. China)
Dr. B. Schneider, Prof. Dr. J. Gershenzon
Max Planck Institute for Chemical Ecology, Jena (Germany)
S.-H. Luo
Graduate School of Chinese Academy of Sciences
Beijing (P. R. China)

[**] This research was supported financially by the "Hundred Talents Program" of the Chinese Academy of Sciences (CAS), the National Natural Science Foundation of China, the State Key Laboratory of Phytochemistry and Plant Resources in West China (P2009-ZZ01 and P2008-ZZ18), the Germplasm Bank of Wild Species, and the CAS Innovation Program of Kunming Institute of Botany (540806321211, 07067722K1, and 07067712K1). We thank Prof. Ji-Kai Liu and Prof. Han-Dong Sun for valuable suggestions on the whole research, Prof. Qi-Tai Zheng and Prof. Ren-Wang Jiang for helpful discussions on the X-ray crystal structure of compound **1**, and Zong-Xin Ren for assistance in the collection of plant material.

Supporting information for this article is available on the WWW under http://dx.doi.org/10.1002/anie.201000449.

broad storage cavity 40–60 μm in diameter (Figure 1D and E), and are abundant on the abaxial leaf surfaces and bracts, but are entirely absent from the adaxial surfaces. Sometimes these trichomes are slightly sunken in the epidermis (Figure 1D and E). The capitate glandular trichomes are particularly abundant on the surfaces of young leaves. They have one or two globular-like storage cavities 10–30 μm in diameter. When there are two storage cavities, they are attached in series to one stalk, with the smaller one pointing up and the larger one down (Figure 1D and F).

Trichome exudates of *L. canum* were collected by brushing, wiping, and a rapid wash with chloroform, as described in the Supporting Information. After the solvent wash, the glandular trichomes appeared very shrunken under the microscope, thus indicating that the majority of their contents had been extracted. TLC analysis of the exudate developed with a nonpolar system (petroleum ether/ethyl acetate, 4:1) showed mainly two bands (Figure S1 in the Supporting Information), which indicated that two lipophilic but relatively nonvolatile compounds **1** and **2** were the major metabolites of the trichomes of *L. canum*, with **2** as the most abundant metabolite (Figure S1 in the Supporting Information).

The amount of trichome extract was insufficient for the isolation and identification of **1** and **2**, and therefore a petroleum ether extract of the whole leaves of *L. canum* was used for this purpose. The extract was separated successively by column chromatography on silica gel, MCI gel, and Sephadex LH-20, and compounds **1** and **2** were finally purified.

Compound **1** was isolated as colorless crystals, and was established to have a molecular formula of $C_{25}H_{36}O_5$ by negative FAB mass spectrometry (FAB-MS) and high-resolution (HR) ESI-MS. The IR spectrum showed absorptions for hydroxy groups and a keto carbonyl group. In the ^{1}H NMR spectrum (Table 1), singlets of four tertiary methyl groups at $\delta_H = 1.31$, 1.76, 1.80, and 1.97 ppm (each 3H) and two doublets of secondary methyl groups at $\delta_H = 0.96$ and 0.86 ppm were clearly shown. Three doublets of olefinic protons at $\delta_H = 5.42$ ($J = 8.7$ Hz), 6.15 ($J = 1.2$ Hz), and 7.21 ppm ($J = 1.2$ Hz) indicated the presence of a trisubstituted double bond and a disubstituted furan ring, deduced from their chemical shifts and coupling pattern. Three one-proton singlets at $\delta_H = 2.47$, 2.69, and 2.79 ppm were ascribable to either methine or free hydroxy groups. Other signals occurred in a relatively high-field region (between $\delta_H = 1.47$ and 2.78 ppm) and mostly overlapped, resonating from either methine or methylene signals.

The ^{13}C NMR and distortionless enhanced polarization transfer (DEPT) spectra exhibited 25 carbon resonances, which consisted of six methyl, four methylene, and eight methine groups, including an oxymethine ($\delta_C = 76.3$ ppm) and three olefinic methine groups ($\delta_C = 112.8$, 119.1, and 139.8 ppm). There were signals of seven quaternary carbon atoms including three oxygenated ones ($\delta_C = 82.8$, 84.8, and 85.8 ppm), three olefinic ones ($\delta_C = 113.6$, 140.0, and 150.3 ppm), and a keto carbonyl carbon atom ($\delta_C =$ 213.1 ppm; Table 1). These data were consistent with the signals observed in the ^{1}H NMR spectrum, and suggested a highly oxygenated sesterterpenoid skeleton for **1**.

Table 1: NMR spectroscopic data of compounds **1** and **2** in $CDCl_3$.[a]

	1[b]		**2**	
Position	δ_H, (J [Hz])	δ_C	δ_H, (J [Hz])	δ_C
1	1.76, s	19.0, q	1.72, s	18.8, q
2	–	140.0, s	–	138.8, s
3	5.42, d (8.7)	119.1, d	5.46, d (9.0)	119.9, d
4	4.60, d (8.7)	76.3, d	4.35, d (9.0)	75.8, d
5	–	84.8, s	–	86.2, s
6	1.87, m	38.9, d	1.87, m	44.8, d
7	2.11, m	49.7, d	1.61, m	45.8, d
8α	1.82, m	29.8, t	1.28, m	28.5, t
8β	2.16, m		1.81, m	
9α	1.50, m	30.6, t	1.31, m	32.1, t
9β	2.01, m		1.93, m	
10	2.22, m	47.1, d	2.11, m	32.8, d
11	–	85.8, s	1.76, m	64.6, d
12	–	213.1, s	–	209.4, s
13	2.69, s	69.3, d	2.74, s	70.7, d
14	–	82.8, s	–	81.9, s
15	2.06, dd (8.1, 8.5)	42.2, t	2.07, t (8.6)	41.4, t
16	2.74, dd (8.1, 8.5)	20.9, t	2.71, t (8.6)	20.6, t
17	–	150.3, s	–	150.5, s
18	–	113.6, s	–	113.4, s
19	6.15, d (1.2)	112.8, d	6.10, d (1.5)	112.7, d
20	7.21, d (1.2)	139.8, d	7.16, d (1.5)	139.6, d
21	1.80, s	26.3, q	1.77, s	26.1, q
22	0.96, d (6.9)	14.2, q	0.94, d (7.0)	13.8, q
23	0.86, d (7.3)	16.6, q	1.14, d (6.5)	21.6, q
24	1.31, s	22.7, q	1.20, s	22.6, q
25	1.97, s	9.8, q	1.93, s	9.7, q

[a] ^{1}H NMR spectra were recorded at 500 MHz; ^{13}C NMR spectra were recorded at 125 MHz. [b] Hydroxy group signals of **1**: $\delta_H = 2.47$ (5-OH), 2.79 ppm (11-OH).

By using a heteronuclear single-quantum correlation (HSQC) experiment, all proton signals (including the methine and methylene signals centered in the high-field region) were unambiguously assigned to their respective carbon atoms except for the two singlets at $\delta_H = 2.47$ and 2.79 ppm, which indicated that these two protons were from free hydroxy groups. In the ^{1}H–^{1}H COSY spectrum, correlations established the coupling relationships of H-3/H-4, Me-22/H-6/H-7/H_2-8/H_2-9/H-10/Me-23, H_2-15/H_2-16, and H-19/H-20. Weak correlations of H-3/Me-1 and Me-21 suggested ^4J couplings between H-3 and the two methyl groups.

In the heteronuclear multiple bond coherence (HMBC) spectrum (Figure S2 in the Supporting Information), the mutual ^{1}H–^{13}C correlations between Me-1 and Me-21 and their simultaneous correlations to C2 and C3, as well as the correlations from H-4 to C2 and C3, indicated the existence of an oxygenated isoprenyl moiety, which was attached to C6 through an oxygenated quaternary carbon atom at $\delta_C =$ 84.8 ppm (C5), judging from the HMBC correlations between 5-OH and C4 and C6. The long-range heterocorrelations from 11-OH to C7, C10, the keto carbon atom, and the oxy-quaternary carbon atom at $\delta_C = 85.8$ ppm indicated this oxy-quaternary carbon atom to be C11, the keto carbon atom to be C12, and the existence of C11/C10, C11/C7, and C11/C12

carbon–carbon connections. Thus, a five-membered ring (ring A) consisting of C7 to C11 was formed. The H-13 singlet showed HMBC correlations with three quaternary carbon atoms, namely C5, C12, and C14, which suggested these were adjacent carbon atoms of C13. Hence, a six-membered ring (ring B) containing C5, C6, C7, C11, C12, and C13 was likely, which was also supported by the HMBC correlation between 5-OH and C13. In addition, linkage of C14 and a furan ring by a $-CH_2CH_2-$ moiety (C15 and C16) could be deduced from HMBC correlations from H_2-16 to C14, C17, and C18. The last two tertiary methyl groups could be positioned at C14 and C18, respectively, owing to the HMBC correlations from one methyl group to C13 and C15, and from the other to C17 and C19. The molecular formula of **1**, which corresponded to eight double-bond equivalents,

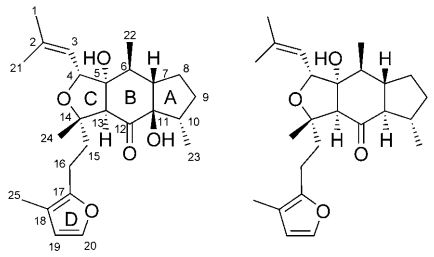

1 **2**

implied the existence of an oxygen bridge in the compound. The absence of 4-OH and 14-OH protons was a hint that the oxygen bridge occurred between C4 and C14. Careful inspection of the HMBC spectrum of **1** revealed a cross-peak between H-4 and C14, although it was not as strong as other correlations. The basic planar structure of **1** was therefore determined.

The relative stereochemistry of all chiral centers in **1** was established by a 2D rotational nuclear Overhauser effect spectroscopy (ROESY) experiment (Figure S3 in the Supporting Information). The observation of ROESY correlations of H-4 with H-7, Me-22, and Me-24, and of 11-OH with H-10 and Me-24 indicated that H-4, H-7, Me-22, Me-24, and 11-OH were in the same orientation (β configuration). Moreover, the ROESY data for 5-OH with H-6, H-13, H_2-15, and H_2-16, and of H-13 with H-6 and Me-23 were also observed, thus leading to assignments of an α configuration to 5-OH, H-6, H-13, Me-23, and the furan-containing side chain connected to C14.

Because **1** is a novel sesterterpenoid possessing such a unique skeleton, X-ray diffraction was necessary to confirm its structure and relative stereochemistry. A single crystal of **1** was successfully obtained from a mixture of petroleum ether/acetone/methanol (1:1:0.1), and X-ray crystallographic analysis was carried out. The result unambiguously established the complete structure and relative configuration of **1** (Figure 2).[7] The structure consists of a cyclopentane ring A, a cyclohexanone ring B, a tetrahydrofuran ring C, and furan ring D. Both rings A/B and B/C are *cis*-fused. Ring A shows a well-shaped envelope conformation with C11 displaced by 0.478 Å from the least-square plane of the remaining four

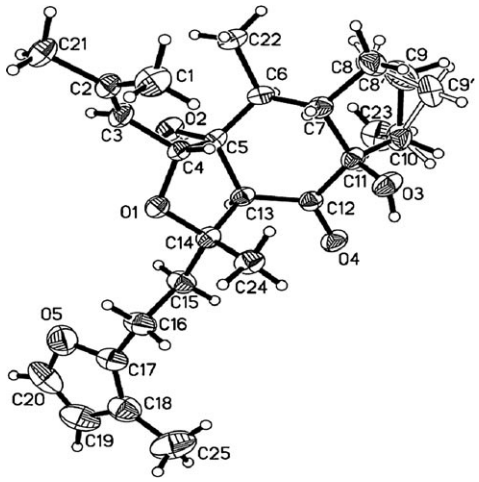

Figure 2. X-ray crystallographic structure of compound **1**, with the atom labeling scheme. Displacement ellipsoids are shown at the 30% probability level.

atoms (C7, C8, C9, C10). Ring B exhibits a twisted half-chair conformation because of the presence of a carbonyl group at C12. Ring C also shows an envelope conformation with C4 displaced by 0.573 Å from the least-square plane of the remaining four atoms (O-1, C14, C13, C5). Ring D is planar and is roughly perpendicular to the least-square plane of ring C with a large dihedral angle of 80.7°. In the solid state, intramolecular and intermolecular hydrogen bonds among the hydroxy groups at C5 and C11 and the carbonyl group are formed. Consequently, compound **1** was determined as shown, and was named leucosceptroid A.

Compound **2** was obtained as a colorless oil with a molecular formula of $C_{25}H_{36}O_4$, as determined by a combination of negative FAB-MS and ^1H and ^{13}C NMR spectra (including DEPT), which was confirmed by HR-ESI-MS. This molecular formula was only one oxygen atom less than that of **1**. The close resemblance between the NMR spectra of **2** (Table 1) and **1** indicated that **2** was another sesterterpenoid structurally similar to **1**. The major difference was the replacement of an oxygenated quaternary carbon atom in **1** by a methine group in **2** ($\delta_C = 64.6$ ppm), which suggests that either C5, C11, or C14 of **2** was not oxygenated. In the HMBC spectrum of **2** (Figure S4 in the Supporting Information), the simultaneous long-range ^1H–^{13}C correlations from H-6 and Me-23 to the carbon atom at $\delta_C = 64.6$ ppm indicated that this methine group was ascribable to C11. Accordingly, compound **2** was identified as an 11-dehydroxy derivative of **1**.

The ROESY spectrum of **2** (Figure S5 in the Supporting Information) also showed a similar correlation pattern to that of **1**, which suggested that the relative configurations of most chiral centers in **2** remained unchanged. However, as a result of the signal overlap of H-11 with H-8β and Me-21, it was not easy to define the stereochemistry of C11 from the ROESY spectrum. A NOE difference experiment was therefore performed. Irradiation of the proton at $\delta_H = 1.14$ ppm (Me-23) induced NOEs at $\delta_H = 1.31$ (H-9α), 2.11 (H-10), and 1.76 ppm (H-11), which indicated that H-11 was α-oriented. In addition, irradiation of Me-24 induced NOEs of H-4 and

H_2-15, irradiation of Me-22 led to enhancement of the signals of H-4 and H-7, irradiation of H-13 resulted in enhancement of the signal H_2-15, and irradiation of H-4 caused the enhancement of signals of H-7, Me-22, and Me-24. All these NOEs were in agreement with the above observations in the ROESY spectrum, thus confirming the relative stereochemistry of **2**. Finally, compound **2** was characterized as shown, and was named leucosceptroid B.

Since the leucosceptroids A (**1**) and B (**2**) are major trichome metabolites of *L. canum*, the exact contents of the two compounds in leaves and trichomes were determined. Quantitative analyses were performed by an HPLC method with the above isolated samples as external standards. As shown in Table 2, the contents of **1** and **2** in leaves were

Table 2: Contents of compounds **1** and **2** in leaves and trichomes.

Sample	Content	
	1	**2**
Fresh leaves ($\mu g\,cm^{-2} \pm SD$)	8.68 ± 0.99	21.48 ± 0.49
Fresh leaves ($\mu g\,mg^{-1} \pm SD$)	0.46 ± 0.02	1.37 ± 0.06
Fresh trichomes ($\mu g\,mg^{-1} \pm SD$)	4.79 ± 0.40	27.88 ± 1.36
Trichome extracts ($\mu g\,mg^{-1} \pm SD$)	54.50 ± 4.85	188.29 ± 4.93

SD = standard deviation.

(8.68 ± 0.99) and (21.48 ± 0.49) $\mu g\,cm^{-2}$, or (0.46 ± 0.02) and (1.37 ± 0.06) $\mu g\,mg^{-1}$ fresh weight, respectively. In fresh trichomes, **1** and **2** constituted (4.79 ± 0.40) and (27.88 ± 1.36) $\mu g\,mg^{-1}$, respectively. Because the trichome samples collected from the surfaces of the leaves for metabolite analysis included not only glandular (both peltate and capitate) trichomes but also nonglandular trichomes, and probably even some dirt, further quantification of **1** and **2** in trichome extracts was carried out. It was found that **1** and **2** accounted for (54.50 ± 4.85) and (188.29 ± 4.93) $\mu g\,mg^{-1}$ of the trichome extracts, respectively (Table 2).

The antifeedant activities of leucosceptroids A (**1**) and B (**2**) to the larvae of two generalist insect herbivores, the beet armyworm (*Spodoptera exigua*) and the cotton bollworm (*Helicoverpa armigera*), were assessed. From the results in Table 3, it was evident that both compounds were potentially a deterrent to the two insects, with an EC_{50} value ranging from 3.78 to 20.38 $\mu g\,cm^{-2}$. The antifungal effects of **1** and **2** against

Table 3: Antifeedant activity and antifungal effects of **1** and **2**.

Test organism	Compound	
	1	**2**
Insect		
Spodoptera exigua (Beet armyworm)	3.78[a]	5.87[a]
Helicoverpa armigera (Cotton bollworm)	20.38[a]	8.36[a]
Fungus		
Colletotrichum musae	42.79 ± 1.78[b]	0.27[c]
Colletotrichum gloeosporioides	ND[b]	0.40[c]
Fusarium oxysporum f. sp. *niveum*	36.36 ± 3.91[b]	0.68[c]
Rhizoctonia solani	20.23 ± 2.81[b]	0.37[c]

[a] EC_{50} ($\mu g\,cm^{-2}$). [b] Inhibition % ($\pm$SD) at 500 μM. [c] EC_{50} (mM). ND = Not determined.

Colletotrichum musae, *C. gloeosporioides*, *Fusarium oxysporum* f. sp. *niveum*, and *Rhizoctonia solani* were also tested. As shown in Table 3, **2** clearly inhibited the growth of the four strains of agricultural pathogenic fungi tested, with EC_{50} values between 0.27 and 0.68 mM (Table 3), respectively. Compound **1**, which differed from **2** only in the presence of an additional OH group, was less active.

Trichomes can serve as a direct physical barrier for plants against enemy attacks by virtue of their size and density. On the other hand, they may also serve as chemical barriers by synthesizing and secreting secondary metabolites. The mode of action of trichome compounds in plant defense is varied, and includes physical immobilization of insects and spores, direct toxicity to insects and fungi, irritant responses to herbivores, and so on.[8] The distribution and morphology of the trichomes of *L. canum* are similar to those found on other Labiatae plants. However, the secondary metabolites harbored by them are unique in nature. Through comparison of the contents of leucosceptroids A (**1**) and B (**2**) in leaves (micrograms per cm^2) with the EC_{50} values of the antifeedant bioassay results, we showed that the levels of sesterterpenoids in leaves are sufficiently high to deter the feeding of generalist insects. In addition, the level of accumulation of sesterterpenoids in trichomes also appears to inhibit pathogenic fungal growth. Thus, it can be suggested that the trichome sesterterpenoids of *L. canum* function in defense against herbivores and pathogens. To the best of our knowledge, this is the first discovery of natural sesterterpenoids with such a unique carbon skeleton, of sesterterpenoids in plant glandular trichomes, and the first time sesterterpenoids have ever been shown to have biological activity against plant-feeding insects and pathogens, and thus demonstrated to be involved in plant defense.

Although it is yet to be experimentally demonstrated, it is highly probable that the sesterterpenoids of *L. canum* are not only accumulated in the glandular trichomes, but also biosynthesized there. Based on the relative sizes of the trichomes and amounts of secretion, the sesterterpenoids are likely to be localized in the peltate glands, with perhaps additional low levels in the smaller capitate glands. A more accurate localization of these sesterterpenoids to type-specific trichomes might be realized through metabolite microprofiling methods, such as laser microdissection (LMD) coupled with NMR spectroscopy and MS,[9] which would shed more light on the ecological function of each individual type of trichome.

Terpenoids are the largest class of natural products with a variety of roles in mediating antagonistic and beneficial interactions among organisms in the natural world.[10] Although sesterterpenoids have been reported from widespread sources, including various marine organisms (especially sponges), terrestrial fungi, lichens, higher plants, and insects,[11] their distribution and natural functions in plants have not been well investigated. It is not even clear how the presumptive precursor, geranylfarnesyl diphosphate (GFPP), is formed in plants, although it has been reported that in some Archaea GFPP synthase was evolved from geranylgeranyl diphosphate (GGPP) synthase.[12,13] Considering the limited distribution, special chemical structures, and broad biological

activities, the biosynthesis and ecological function of natural sesterterpenoids in plants are worthy of further attention.

The sesterterpenoids previously reported from a *L. canum* collection from Nepal[14,15] are quite distinct from those described here for plants of Chinese origin. This might be caused by either environmental or genetic differences leading to altered expression of the enzymes responsible for the cyclization of GFPP. In this regard, the characteristic sesterterpenoids may also be of important chemotaxonomic significance for *L. canum* and even for the genus *Leucosceptrum*.

L. canum contains other constituents of chemical and ecological interest. The compounds responsible for its colored nectar are currently being investigated in our laboratory.

Experimental Section

Experimental procedures, plant materials, extraction and isolation of compounds **1** and **2**, microscopy, collection of trichome exudates and metabolite analysis, quantification of sesterterpenoids in trichomes and trichome extracts, bioassays of sesterterpenoids, TLC of trichome metabolites, ^{1}H and ^{13}C NMR spectra, and HMBC and ROESY correlations of **1** and **2** are given in the Supporting Information.

Important data of leucosceptroid A (**1**): Colorless crystals; m.p. 186–188 °C; $[\alpha]_D^{19} = +151.13$ ($c = 0.3$, $CHCl_3$); UV ($CHCl_3$) λ_{max} ($\log\varepsilon$): 240 (3.15), 202 (2.82) nm; IR (KBr): $\tilde{\nu} = 3456, 2963, 2874, 1680, 1509, 1447, 1384, 1273, 1239, 1140, 1063, 1023, 909, 749\ cm^{-1}$; negative FAB-MS: m/z (%): 569 (100) $[M+MNBA]^-$, 415 (83) $[M-H]^-$, 387 (17), 339 (10), 224 (16), 211 (18), 96 (11); HR-ESI-MS: m/z: 451.2245 $[M+Cl]^+$ (m/z_{calcd} $[C_{25}H_{36}O_5Cl]^+ = 451.2251$); ^{1}H and ^{13}C NMR, see Table 1.

Important data of leucosceptroid B (**2**): Colorless oil; $[\alpha]_D^{19} = +55.50$ ($c = 0.9$, $CHCl_3$); UV ($CHCl_3$) λ_{max} ($\log\varepsilon$): 240 (3.06) nm; IR (KBr): $\tilde{\nu} = 3442, 2962, 2934, 2870, 1702, 1452, 1376, 1276, 1150, 1052, 983, 727\ cm^{-1}$; negative FAB-MS m/z (%): 399 (20) $[M-H]^-$, 381 (59), 279 (100), 255 (20), 141 (24); HR-ESI-MS: m/z: 435.2297 $[M+Cl]^+$ (m/z_{calcd} $[C_{25}H_{36}O_4Cl]^+ = 435.2302$); ^{1}H and ^{13}C NMR, see Table 1.

Received: January 26, 2010
Published online: May 10, 2010

Keywords: antifeedant agents · antifungal agents · natural products · sesterterpenoids · structure elucidation

[1] G. J. Wagner, E. Wang, R. W. Shepherd, *Ann. Bot.* **2004**, *93*, 3–11.
[2] R. G. Kelsey, G. W. Reynolds, E. Rodriguez, *The Chemistry of Biologically Active Constituents Secreted and Stored in Plant Glandular Trichomes*, Plenum, New York, **1984**.
[3] D. McCaskill, R. Croteau, *Nat. Biotechnol.* **1999**, *17*, 31–36.
[4] H. Peng, Z.-Y. Wu, *Acta Bot. Yunnanica* **2001**, *23*, 278–286.
[5] D. M. Hansen, J. M. Olesen, T. Mione, S. D. Johnson, C. B. Muller, *Biol. Rev.* **2007**, *82*, 83–111.
[6] J. Chen, *Leucosceptrum Smith*, *Vol. 66*, Academic, **1977**, pp. 301–304.
[7] CCDC 763172 (**1**) contains the supplementary crystallographic data for this paper. These data can be obtained free of charge from The Cambridge Crystallographic Data Centre via www.ccdc.cam.ac.uk/data_request/cif. Crystal data of **1**: $C_{25}H_{36}O_5$, $M = 416.54$, colorless block, size $0.30 \times 0.13 \times 0.10\ mm^3$, orthorhombic, space group $P2(1)$, $a = 13.207(3)$, $b = 6.2398(15)$, $c = 15.664(4)$ Å, $\alpha = 90$, $\beta = 114.93$, $\gamma = 90°$, $V = 1170.6(5)$ Å^3, $T = 25$ °C, $Z = 2$, $d = 1.182\ g\,cm^{-3}$, $\mu(Mo_{K\alpha}) = 0.71073$ Å, $F(000) = 452$, 6735 reflections in $h(-13/16)$, $k(-8/7)$, $l(-20/16)$, measured in the range $1.43° \le \theta \le 28.29°$, completeness $\theta_{max} = 95.2\,\%$, 2711 independent reflections, $R_{int} = 0.0872$, 925 reflections with $Fo > 4\sigma(Fo)$, 293 parameters, 31 restraints, $R1_{obs} = 0.0477$, $wR2_{obs} = 0.0718$, $R1_{all} = 0.1689$, $wR2_{all} = 0.0968$, GOF = 0.725, Flack parameter −4.1(18), largest difference peak and hole = 0.124 and −0.140 e Å^3. The crystal structure of **1** was solved by a direct method using the program SHELXS-97 (G. M. Sheldrick, *SHELXS97 and SHELXL97*, University of Göttingen, Germany, **1997**) and subsequent Fourier difference techniques, and refined anisotropically by full-matrix least squares on F^2 using SHELXL-97 (G. M. Sheldrick, *SHELXTL*, Version 6.10, Bruker AXS Inc., Madison, Wisconsin, USA, **2000**).
[8] E. M. Wang, R. Wang, J. DeParasis, J. H. Loughrin, S. S. Gan, G. J. Wagner, *Nat. Biotechnol.* **2001**, *19*, 371–374.
[9] S. H. Li, B. Schneider, J. Gershenzon, *Planta* **2007**, *225*, 771–779.
[10] J. Gershenzon, N. Dudareva, *Nat. Chem. Biol.* **2007**, *3*, 408–414.
[11] Y. Liu, L. Wang, J. H. Jung, S. Zhanga, *Nat. Prod. Rep.* **2007**, *24*, 1401–1429.
[12] A. Tachibana, *FEBS Lett.* **1994**, *341*, 291–294.
[13] A. Tachibana, Y. Yano, S. Otani, N. Nomura, Y. Sako, M. Taniguchi, *Eur. J. Biochem.* **2000**, *267*, 321–328.
[14] M. L. Choudhary, R. Ranjit, Atta-ur-Rahman, T. M. Shrestha, A. Yasin, M. Parvez, *J. Org. Chem.* **2004**, *69*, 2906–2909.
[15] M. Q. Choudhary, R. Ranjit, Atta-ur-Rahman, S. Hussain, K. P. Devkota, T. M. Shrestha, M. Parvez, *Org. Lett.* **2004**, *6*, 4139–4142.

